Mausam, (1995), **46**, 4, 367-376

551.511 : 551.551.531.43 : 551.50

Effects of change in orientation and surface roughness of terrain on thermally induced upslope flows in western Ghats : A numerical study

M. TIWARI and N. RAMANATHAN
Indian Institute of Technology, New Delhi
(Received 9 June 1994, Modified 10 February 1995)

सार — एक द्विआयामी मेसोस्केल निदर्श का प्रयोग करते हुए दिन के समय आरोही प्रवाह पर स्थल की सतही स्थूलता तथा अवस्थिति में परिवर्तन के प्रभाव की जांच की गई है। इस उद्देश्य के लिए पश्चिमी घाट के वास्तविक पर्वत-विज्ञान पार्श्वचित्र का चयन किया गया। इसमें सूर्योदय से लेकर बारह घंटे तक समाकलन किए गए हैं। संख्यात्मक अनुसरण से यह पता चलता है कि स्थल की अवस्थिति में परिवर्तन से आरोही प्रवाह की तीव्रता व्यवहारिक रूप से अप्रभावित रहती है। तथापि स्थूलता के विस्तार में वृद्धि से प्रवाह की तीव्रता में कमी होती है। तुलना के दृष्टिकोण से ढलान कोणों में परिवर्तन के साथ पूर्व अनुसंधानकर्ताओं के परिणामों की जांच की गई है।

ABSTRACT. The effect of change in orientation and surface roughness of terrain on the daytime upslope flow is investigated using a 2-dimensional mesoscale model. A realistic orography profile of western ghat is chosen for the purpose. Twelve hour of integrations are performed starting from sunrise. The numerical simulation have shown that the intensity of upslope flows remained practically unaffected by change of orientation of terrain. However, increase in roughness length decreases the intensity of developed flows. For comparison purposes, the results of previous investigators are verified with a change in slope angles.

Key words — Upslope flow, Surface roughness, Western Ghat studies.

1. Introduction

In a region with irregular terrain, local wind patterns can develop because of the differential heating between the ground surface and the free atmosphere at the same elevation some distance away. A large diurnal temperature variation usually occurs at the ground, so that during the day the higher terrain becomes an elevated heat source, whereas at night, it acts as an elevated heat sink. During daytime, warm and moist air moves towards high elevation (upslope wind), but during the night, cool and dense air moves down the slope of terrain (downslope wind or nocturnal drainage flow). These circulations are localized and can be easily detected if the prevailing flow is weak.

In many situations, daytime induced thermal circulation along terrain slopes plays a major role in determining local weather and pollution dispersion. Numerous observational and modelling studies have been carried out to evaluate these circulations. Mahrer and Pielke (1977), McNider and Pielke (1981), Banta (1986), have simulated various aspects of upslope and downslope winds using numerical models. Either hydrostatic or non-hydrostatic mesoscale models are used to simulate such circulations. Most of the above mentioned studies deal with situations typical to mid-latitude regions. However, there are very few systematic studies related to the simulation of airflow over an irregular terrain in India.

Hilly terrain covers western parts of peninsular India. The slope winds developed due to the differential heating over the terrain have to be examined for proper understanding of the local weather at those places. The impact of background atmospheric thermal stability and slope steepness on the daytime thermally induced upslope flow was investigated in detail using analytical and numerical model approaches (Ye *et al.* 1987). Panofsky and Townsend (1964) Wagner (1966) studied the distribution of wind with height in hydrostatically neutral air for a changing terrain roughness, but the effect of change of orientation of terrain and surface roughness on the intensity of upslope flows were not studied. The purpose of the present investigation is to study the development of upslope flows over western Ghats and the impact of orientation of terrain and surface roughness on these circulations.

An attempt has been made to study the sensitivity of the upslope flow to various terrain features using a 2-dimensional mesoscale model. The conclusion drawn from this study is expected to lead to a better understanding of the development of local weather at a specific location in India.

TABLE 1

Initial θ, q and T_{soil} values at different model levels

Levels z^* (m)	θ (°K)	q (g/kg)	T_{soil} (°K) (5 cm interval)
2	300.2	0.019	299.6
20	300.3	0.019	299.6
50	300.4	0.019	299.7
100	300.6	0.0188	299.8
300	301.4	0.0185	299.9
500	302.5	0.018	300.1
1000	306.0	0.015	300.4
1500	308.6	0.013	300.6
2500	314.2	0.010	301.6
3500	318.8	0.001	302.5
5000	324.0	0.001	302.4
6500	326.4	0.0001	301.7
8000	331.4	0.0001	301.1
9000	336.4	0.0001	300.6
10000	341.4	0.0001	300.4

TABLE 2

Model input parameters

Day of the year	= 1 April, 1969
Latitude	= 19° N
Albedo of the surface	= 0.2
Soil wetness	= 0.05
Soil conductivity	= 0.003 cm^2/s
Soil density	= 1.5 g/cm^3
Soil specific heat	= 0.32 cal/g/K
Surface pressure	= 1013 hPa
Time step (Δt)	= 60 sec
Grid interval (Δx)	= 6 km
Large scale surface temperature	= 300°K

2. Model description

The model used in the present study is a 2-dimensional version of the mesoscale model, developed by Pielke (1974a) and modified subsequently by Mahrer and Pielke (1977a), Mahrer and Pielke (1978) and McNider and Pielke (1981). This model has been adopted and further modified to simulate mesoscale circulations over the Andaman Islands (a chain of islands in the Bay of Bengal) by Kar and Ramanathan (1987).

The model is hydrostatic, and has terrain following co-ordinate system. Transformation of the governing equations from cartesian to terrain following co-ordinate is carried out using the shallow slope approximation (Pielke and Martin 1981). The vertical co-ordinate is of the form

$$Z^* = S\,\frac{Z - Z_g}{S - Z_g} \qquad (1)$$

here S and S are the initial and instantaneous heights of the material surface and Z_g the ground elevation above sea level. The basic equations of the model are given in the Appendix. A brief selective summary of the model is given below.

(a) *Boundary Layer*

The calculation of surface fluxes of momentum, heat and moisture are based on the works of Businger (1973). The exchange coefficients in the PBL above surface layer utilize O'Brien's (1970) functional form while the PBL height is predicted for unstable conditions using Deardorff (1974) prognostic equation. For stable conditions, Smeda (1979) prognostic equation is used (Eqn. 9 or 10 given in Appendix). The roughness parameter over the land is prescribed.

(b) *Surface Heat Balance*

The temperature at soil-air interface is calculated using a heat balance equation for solar radiation, incoming and outgoing longwave radiation, turbulent heat fluxes.

(c) *Radiation*

The changes of air temperature due to shortwave and longwave radiation flux divergence are parameterized following the method of Atwater and Brown (1974). Heating of the atmosphere by solar radiation is confined to water vapour, while carbondioxide and water vapour are considered in the longwave radiation heating and cooling algorithm.

(d) *Numerical aspects*

The governing hydrostatic equations of motion, heat, moisture and continuity are approximated in finite difference form using 60 sec time step alongwith horizontal grid interval of 6 km. A very accurate Lagrangian spline scheme is used for advection term, which is discussed by Mahrer and Pielke (1978). In the vertical, the atmosphere upto model top (10 km) is divided into 15 levels as shown in Table 1. Starting at sunrise, the model was integrated for 12 hours.

(e) *Initialization*

The initial wind velocity above the initial specified PBL is taken geostrophically balanced. To obtain initial wind field within the PBL, the balance between the pressure gradient, Coriolis and turbulent friction forces are obtained by integrating the steady state Ekman equations over six inertial periods. Above the PBL, the observed wind value were used. The entire domain was initialized with the same wind values to avoid spurious accelerations.

Hydrostatic assumption is appropriate since the ratio of vertical (h) to horizontal (L) scale of circulation, studied here is substantially less than unity (Pielke and Martin 1981). Incompressible condition is also satisfied as the ratio of vertical scale to scale height (H) of the atmosphere is less than 1. The model domain is 21 × 15 grid with horizontal extent 260 km and vertical 10 km. Zero gradient boundary conditions are specified at both the lateral boundaries of the model

$$W^* = \frac{\partial}{\partial X}(u,\ v,\ \theta,\ q,\ \pi,\ S,\ Z_g) = 0 \qquad (2)$$

at $X = 0$ and $X = L_1$

where,

L_1 is the horizontal extent of X co-ordinate in the model.

At the model top ($Z^* = \overline{S} = 10$ km):

$u = u_g,\ v = v_g,\ w^* = 0$

$\theta\ (\overline{S})$ = constant., $q\ (\overline{S})$ = constant.

At the bottom ($Z^* = Z_0$):

$u = v = w^* = 0$

$$q_g = F_w\, q_{g\ \mathrm{sat}} + (1 - F_w)\, q\,(1) \qquad (3)$$

where,

F_w = soil wetness

$q\,(1)$ = specific humidity at the first grid level above the surface

$q_{g\ \mathrm{sat}}$ = saturation specific humidity at the ground

3. Initial data used

The initial data used is for summer time conditions. Weak prevailing synoptic flow condition is taken so that the upslope flow can be distinctly distinguished in the simulations. The initial θ, q and T_{soil} values at different depths, as used in the mesoscale model for initialisation are given in Table 1. For higher levels (6.5 km and above) a very low value of specific humidity is prescribed because no data is available in these levels and moisture content at those levels are very low. For T_{soil} 15 levels below the ground at equal depth of 5 cm is taken.

The other inputs to the model are given in Table 2.

For the orography profile of western Ghats, an analytical expression used by Sarker (1965) is chosen. It is represented as:

$$\xi(X) = \frac{a^2 b}{a^2 + x^2} + a' \arctan\left(\frac{x}{a}\right) \qquad (4)$$

where,

$\xi\,(X)$ = elevation of the ground surface at the level $z = -h$, $h = 0.25$ km, a = 18 km, $b = 0.52$ km.

$$a' = (2/\pi) \times 0.35 \text{ km} \qquad (5)$$

In the west to east direction, its height gradually rises to 0.8 km in a distance of 65 km and then ends in plateau of average height 0.6 km. The slope of the mountain is 1.4°.

4. Experiments

(a) In order to compare the results of present investigation with the results of Ye *et al.* (1987), two different types of terrains with different slopes, *viz.*, Gaussian profile and slope plateau were chosen. The initial flow direction was westerly and surface roughness length was taken to be 4 cm. All the other

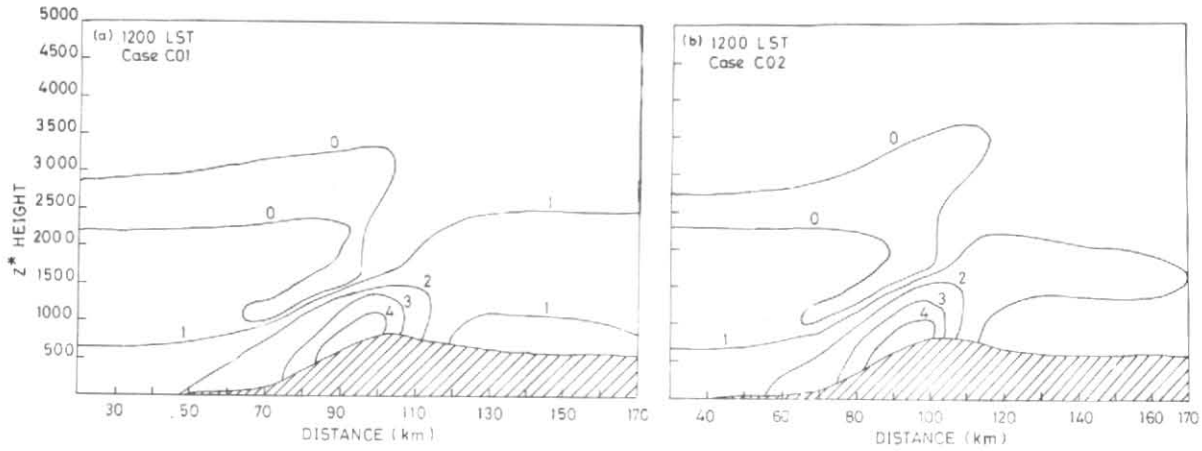

Figs. 1 (a & b). Vertical cross-section presenting the model-simulated u at 1200 LST for case (a) CO1 and (b) CO2

model input parameters were kept same for the following cases, *viz.*,

(*i*) Case I1 : Gaussian profile with slope steepness 1.1°.

(*ii*) Case I2 : Slope plateau, with slope steepness 1.9°

(b) To study the eff ct of change of orientation of terrain, the initial flow direction was altered as below.

(*i*) Case CO1 : Initial flow vesterly

(*ii*) Case CO2 : Initial flow south-westerly

The terrain profile chosen for these cases was the western Ghat profile. The purpose of selecting a south-westerly and westerly flow is to study the development of upslope wind circulation over the region during summer season.

(c) To study the effect of change of roughness length on the developed upslope flows the following cases were considered :

(*i*) Case CS1 : surface roughness length = 4 cm

(*ii*) Case CS2 : surface roughness length = 10 cm

(*iii*) Case CS3 : surface roughness length = 15 cm

(*iv*) Case CS4 : surface roughness length = 50 cm

(*v*) Case CS5 : surface roughness length = 100 cm

The above experiments were performed with the specification of the western Ghat profile given above.

5. Results and discussion

(a) All the model simulations started from sunrise and terminated at sunset. The initial values of θ, q, T_{soil} and other parameters used for the initialisation of the model are given in Tables 1 & 2. After two hours of simulation, the land surface in the model was heated and the upslope circulation began to develop. The values of some of the important parameters u_{max} (maximum of upslope wind speed at the middle of the slope), u^*_{max} (the maximum upslope wind speed within the simulated cross section), θ (1) (the potential temperature at the first model level), Δθ (the difference between the potential temperature at the middle of the slope and corresponding potential temperature at the same elevation in the free atmosphere) for the cases I1 and I2 at selected hours are shown in Table 3. It shows that daytime thermally induced upslope flow intensifies when the terrain slope becomes steeper, *i.e.*, in case I2. The difference between u_{max} and u^*_{max} is more for steeper slopes. These results show similar variations when compared with the results of Ye *et al.* 1987. This served as a check for the correctness of our simulations.

(b) *Dependency of upslope flow intensity on change of orientation of terrain*

The cases CO1 and CO2 which refer to the directional changes of initial flow, which is equivalent to

TABLE 3

Some of the important parameters for the cases I1 and I2

Hour (LST)	Slope angle	u_{max} (m/s)	$\theta(1)$ (°K)	$\Delta\theta$ (°K)	u^*_{max} (m/s)
1200	1.1°	3.6	306.6	2.0	3.8
	1.9°	4.5	306.8	2.8	5.1
1400	1.1°	4.8	308.3	1.7	4.9
	1.9°	5.8	308.2	2.2	6.9

TABLE 4

Values of some of the important parameters at the middle of the slope for the cases CO1 and CO2

Hour (LST)	Initial flow	u_{max} (m/s)	$\theta(1)$ (°K)	$\Delta\theta$ (°K)	h_θ (m)	u^*_{max} (m/s)
1200	S-Wly	3.80	306.5	2.4	1147	4.89
	Wly	3.87	306.4	2.4	1132	5.01
1400	S-Wly	5.19	308.3	2.1	1652	6.44
	Wly	5.09	308.1	2.0	1567	6.43
1600	S-Wly	5.49	309.6	2.0	1995	6.56
	Wly	5.48	309.4	2.0	1890	6.64

the different orientation of terrain are studied. The results at the middle of the slope are tabulated in Table 4. It is clear from this table that the intensity of developed flows remains almost the same at all the hours in both the cases, showing thereby that the change in the direction of initial flow has no significant impact on the developed wind speed or the height of developed PBL. This clearly shows that developed flows are mainly thermally induced and are not governed by the initial flow as expected, since a near zero synoptic flow was used for the start of the simulations. Typical spatial variations of the developed wind speeds (u) for the above cases are shown in Figs 1 (a & b) at the time of maximum surface temperatures, *i.e.,* at 1200 LST. The pattern remains almost the same at all the hours except with a slight change in intensity. These are omitted here for brevity. The simulated vertical profiles of the horizontal velocity u at 1200 LST at the middle of the slope for cases CO1 and CO2 are shown in Fig. 2. It shows that the horizontal velocity u is maximum at 50 m in both

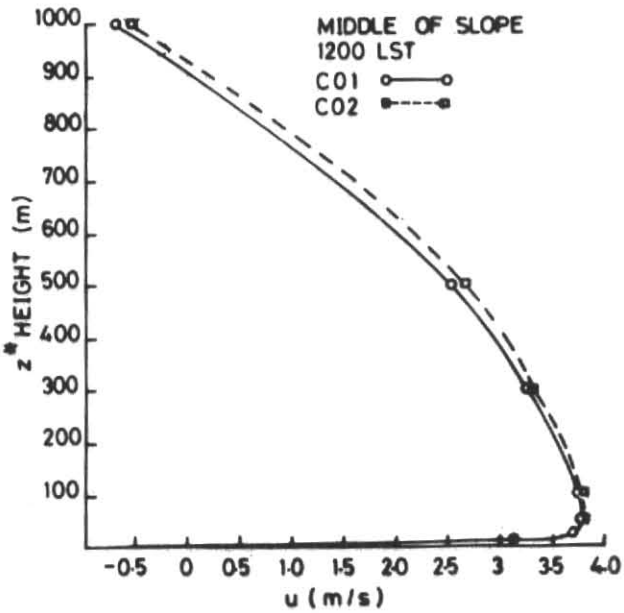

Fig. 2. u-velocity vertical profile at 1200 LST at the middle of slope for the cases CO1 and CO2

the cases. Also, from this figure it is evident that there is almost no difference in the u-profile for these cases. From the results given in Table 4, it is clear that the depth of PBL or other remaining parameters such as θ (1), $\Delta\theta$ etc. are independent of the initial direction of flow or the change of orientation of terrain.

(c) *Dependency of upslope flow intensity on surface roughness lengths*

With all the other input parameters kept unchanged the surface roughness length of the terrain was altered and a number of experiments, as given in section 4, were performed. Under same environmental conditions, due to different surface roughness lengths, the partitioning of thermal energy between sensible and latent heat fluxes is likely to be different. The intensity of day time thermally induced upslope flows is directly related to the magnitude and horizontal distribution of the surface sensible heat fluxes. Therefore, the characteristics of these circulations are likely to get modified for different surface roughness lengths. In view of these facts different cases as mentioned in the previous section were studied. The higher surface roughness lengths over the terrain, *viz.,* 50 and 100 cm were taken since the terrain is usually covered with forest. But in these cases the lowest level of the model has been raised to 50 m so that it is well above the height

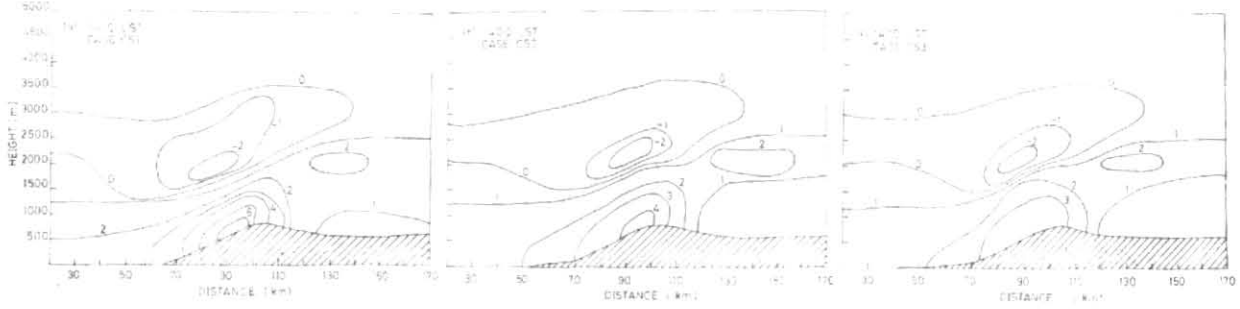

Figs. 3 (a-c). Vertical cross-section presenting the model-simulated u at 1400 LST for the case (a) CS1, (b) CS2 and (c) CS3

of the canopy corresponding to these surface roughness lengths.

The spatial distribution of u at 1400 LST for different surface roughness lengths is shown in Figs. 4, 5 and 6. These show that the intensity of upslope circulation decreases with the increase in surface roughness length. For example, with $z_o = 4$ cm, the maximum velocity developed is nearly 6.0 m/s as in Fig. 3 (a) and with $z_o = 10$ cm the intensity decreases to 4.0 m/s as seen from Fig. 4 (b). From Fig. 4 (c), a further reduction in u, with increase in z_o can be noticed. Typical numerically simulated values of u are given in Table 5.

Ye *et al.* (1987) have obtained an analytical solution for the Prandtl equations under steady state conditions under the prescribed θ and for the parabolic distribution of K-profile. K has got a parabolic profile within PBL.

$$K = K_o \; z(1 - z/h) \tag{6}$$

where, K_o is a constant taken to be equal to 1.1 $k_o u_*$. This type of profile has its maximum at $z = h/2$ and analogous to cubic polynomial profile of O'Brien (1970) used also in the Pielke's (1978) numerical model. The mathematical solution is given by Ye *et al.* (1987),

$$u = \frac{\lambda Q_s \sin\alpha}{2K_o}\left[\ln\left\{\frac{\zeta\,(1-\zeta)}{z_o(1-\zeta_o)}\right\} - (1-2\zeta_o) \times \frac{\ln\left(\dfrac{1-\zeta}{\zeta}\right)}{\ln\left(\dfrac{1-\zeta_o}{\zeta_o}\right)} - 2\zeta + 1\right] \tag{7}$$

where, $\zeta = z/h$

$\zeta_o = z_o/h$

$Q_s = h\;\Delta\theta/2$

$\lambda = g/\theta_o$

and α is the angle of terrain slope.

Typical calculated values of u with the above formulation and the numerically simulated values are given in Table 6. The tabulated results show that with the increase in roughness length (z_o), u decreases with height and has smaller magnitudes at the same level. Above $z = 20$ m, the calculated numerical solution has smaller magnitudes as compared to the analytical solutions for all z_o. Above 1 km, the numerical model results show the velocities change in sign thereby showing a return flow. The apparent discrepancies between the analytical and numerical solutions can be attributed due to different profile formulations for the eddy diffusivity coefficient K. The O'Brien formula for the maximum value of K occurs at $z = h/3$ which is consistent with the observational results of Sato (1981), who found the largest values of K within the region,

$$0.15 < z/h < 0.5$$

although the precise value varied with season and topography. In the analytical formulation used by Ye *et al.* (1987), K_z has been taken to be the quadratic polynomial which is maximum at $h/2$. Wagner (1966) has obtained analytical solutions for the steady state Ekman equations when,

$$K_z = k\; u_* \; (z + z_o) \tag{8}$$

TABLE 5

Typical numerically simulated values of u for cases CS1 and CS3 at 1400 LST

z^* Height (m)	case CS1 (z_0 = 4cm) u (m/s)	case CS3 (z_0 = 15cm) u (m/s)
2.0	4.11	2.73
20.0	4.97	3.54
50.0	5.17	3.69
100.0	5.19	3.74
300.0	4.78	3.53
500.0	4.23	3.23
1000.0	1.93	1.74

for four roughness parameter values 1, 2, 5 and 10 cm. With increase in roughness length the calculated u values show a decrease with increase in roughness length within the PBL. The magnitude of difference between the analytical and numerical increases with increase in roughness length. Our numerical solutions agree with the above results qualitatively. O'Brien's profile used in the Pielke's model, also used in the several boundary layer studies, is known to simulate accurate solutions for a convective boundary layer. Hence, our numerical model results can be taken more accurate than the one calculated by the analytical formulation of Ye *et al.* (1987). It will be interesting to compare the simulated vertical velocities with different orographic profiles. As mentioned previously, the western Ghat profile taken in this study is a combination of a Gaussian profile with a slope-plateau profile so with these profiles in consideration the simulation results are tabulated in Table 7. In the tabulated results the values of w at the middle of the slope are shown. As mentioned, I1 and I2 case results (Table 3) show that an increase in slope steepness induces a more intense circulation as revealed by increase in wind speed (u), vertical velocity etc. Thus, higher convergence and rainfall amounts are possible with increase in slope angle [an indirect verification of Rao (1976) results].

A typical simulated vertical velocity pattern over western Ghats with roughness length of 100 cm is shown in Figs. 4 (a-c). Over the slope-plateau and Gaussian profile for the same roughness lengths, similar patterns were found and the vertical velocities developed are also of the same order.

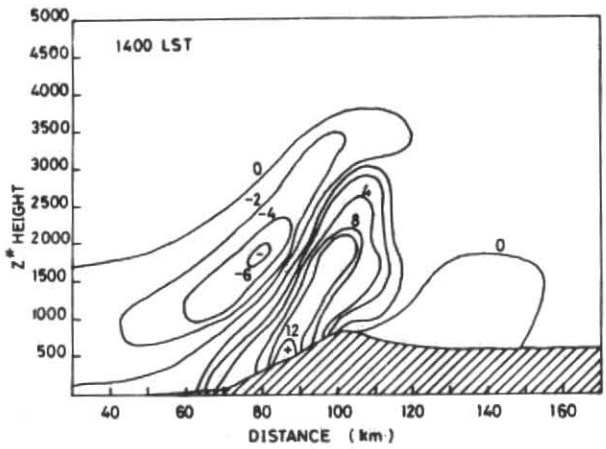

Fig. 4. Typical simulated vertical velocity (w) pattern over western Ghat with z_0 = 100 cm

With decrease in roughness lengths, the simulated vertical velocities are more corresponding to increase in wind speed (u).

6. Conclusions

The major conclusions drawn from the present study are :

(*i*) With the weak initial synoptic flow, the intensity of developed wind speeds over the slopes does not depend on the orientation of slopes with respect to the incident flow. This is shown by cases CO1 and CO2 results. The characteristics of the developed upslope flows, such as, depths of PBL, the maximum wind speeds developed etc. remain practically unaltered.

(*ii*) Roughness length is an important parameter in altering the intensity of upslope flows which is in conformity with Sud *et al.* (1994) results who have shown that roughness length directly affects the aerodynamic resistance, thereby surface stress and momentum flux.

(*iii*) The simulated results differ from the analytical results of Ye *et al.* (1987) due to change in the specification of eddy diffusivity (K) profile.

(*iv*) The intensity of upslope flows with different terrain profiles but with same

TABLE 6

Numerical and analytical results of u (m/s) for typical roughness lengths at 1200 LST

z^* Ht. (m)	case CS1 z_0 = 4cm u (m/s)		Case CS3 z_0 = 15cm u (m/s)		z^* Ht. (m)	case CS5 z_0 = 100cm u (m/s)	
	Numerically simulated	Calculated	Numerically simulated	Calculated		Numerically simulated	Calculated
2.0	3.15	2.84	2.30	1.54	50.0	1.62	1.75
20.0	3.71	4.49	2.92	2.89	60.0	1.65	1.83
50.0	3.80	5.10	3.00	3.39	80.0	1.68	1.94
100.0	3.77	5.52	3.01	3.73	100.0	1.69	2.02
300.0	3.24	5.96	2.72	4.05	300.0	1.37	2.32
500.0	2.55	5.93	2.27	3.98	500.0	0.88	2.33
1000.0	−0.71	4.92	−1.14	0.66	1000.0	−1.09	1.85

steepness and lengths of slopes do not alter the characteristics of developed flows. This result will be of some importance in many areas with irregular terrain.

Future outlook

In our simulations we assumed that the roughness length specified is same for momentum, heat and moisture. However, Garratt and Hicks (1973), Garratt (1978), Beljaars and Holtslag (1991) have shown that the roughness length for momentum is much larger than heat and moisture. A consideration with different roughness lengths will complicate the similarity theory used in our present study. However, the gross features may yet remain unaffected. A study for katabatic flows with different surface roughness lengths specified will be of interest. For simplicity, in our simulation, the contribution of the turbulent fluxed by vegetation is omitted. However, it is known that the vegetation enhances turbulence as shown by Kar and Ramanathan (1987).

TABLE 7

Typical numerically simulated values of w at 1200 LST

z^* Height (m)	Gaussian (slope = 1.1°)	Slope-Plateau (slope = 1.9°)	Western Ghat (slope = 1.4°)
	w (cm/s)	w (cm/s)	w (cm/s)
2.0	10.4	13.3	11.1
20.0	12.2	15.6	13.1
50.0	12.4	15.7	13.4
100.0	12.0	15.0	12.9
300.0	9.3	10.5	9.8
500.0	5.7	6.4	6.2
1000.0	−5.9	−9.2	−6.2

Acknowledgement

The computations were performed in ICL-3980 IIT computer. We thank the authorities for providing the necessary facilities.

References

Atwater, M. A. and Brown, P. Jr., 1974, "Numerical calculation of the latitudinal variation of solar radiation for an atmosphere of varying opacity," *J. Appl. Meteor.*, **13**, 289-297.

Banta, R. M., 1986, "Daytime boundary layer evolution over mountainous terrain Part 2: Numerical studies of upslope flow duration," *Mon. Weath. Rev.*, **114**, 1112-1130.

Beljaars, A. C. M. and Holtslag, A. A. M., 1991, "Flux parameterization over land surfaces for atmospheric models," *J. Appl. Meteor.*, **30**, 321-341.

Businger, J. A., 1973, Turbulent transfer in the atmosphere surface layer, "Workshop in the Micrometeorology", Boston, Am. Meteorol. Soc., 392 p.

Deardoff, J. W., 1974, "Three dimensional numerical studies of the height and mean structure of a heated planetary boundary layer", *Boundary layer Meteor.*, 7, 81-106.

Garratt, J. R., 1978, "Transfer characteristics for a heterogeneous surface of large aerodynamic roughness," *Quart. J. R. Met. Soc.*, **104**, 491-502.

Garratt, J. R. and Hicks, B. B., 1973, "Momentum, heat and water vapour transfer to and from natural and artificial surfaces", *Quart. J. R. Met. Soc.*, **99**, 680-687.

Kar, S. C. and Ramanathan, N., 1987, "Characteristics of airflow over Andaman Island including precipitation," Proc. Indian Acad. Sci., **96**, 169-188.

McNider, R. T. and Pielke, R. A., 1981, "Diurnal boundary layer development over sloping terrain," *J. Atmos. Sci.*, **32**, 2198-2212.

Mahrer, Y. and Pielke, R. A., 1977a, "A numerical study of airflow over irregular terrain," *Contri. Atmos. Phys.*, **50**, 98-113.

Mahrer, Y. and Pielke, R. A., 1978, "A test of an upstream spline interpolation technique for the advective terms in a numerical mesoscale model," *Mon. Weath. Rev.*, **106**, 818-830.

O'Brien, J. J., 1970, "A note on the vertical structure of the eddy exchange coefficient in the planetary boundary layer", *J. Atmos. Sci.*, **27**, 1213-1215.

Panofsky, H. A. and Townsend, A. A., 1964, "Change of terrain roughness and the wind profile," *Quart. J. R. Met. Soc.*, 147-155.

Pielke, R. A., 1974a, "A 3-dimensional numerical model of the sea breeze over South Florida, "*Mon. Weath. Rev.*, **102**, 115-139.

Pielke, R. A. and Martin, C. L., 1981, "The derivation of a terrain following coordinate system for use in hydrostatic model," *J. Atmos. Sci.*, **38**, 1707-1713.

Rao, Y. P.,1976, Southwest Monsoon, Meteorological Monograph, India Met. Dept., 376 p.

Sarker, R. P., 1965, "A theoretical study of mountain waves on Western Ghats," *Indian. J. Met. Geophys.*, **16**, 565-585.

Sato, J., 1981, "Some aspects of diurnal variation and profile of vertical turbulent diffusivity in the atmospheric boundary layer," *Pap. Meteor. Geophys.*, **32**, 247-256.

Smeda, M., 1979, "Incorporation of planetary boundary-layer processes into forecasting models," *Boundary Layer Meteor.*, **16**, 115-129.

Sud, Y. C., Walker, G. K., Kim, J. H., Liston, G. E., Sellers, P. J. and Lau, W. K. M., 1994, "A simulation study of the importance of surface roughness in the tropical deforestation," TROPMET, 1994, IITM, Pune.

Wagner, N. K., 1966, "A two-dimensional time dependent numerical model of Atmospheric Boundary Layer flows over inhomogeneous terrain," Ph. D Thesis, University of Hawaii, 80 p.

Ye, Z. J., Segal, M. and Pielke, R. A., 1987, "Effects of atmospheric thermal stability and slope steepness on the development of thermally induced upslope flow," *J. Atmos. Sci.*, **44**, 3341-3354.

APPENDIX

Model equations

The governing equations of the model are written with the following vertical co-ordinates :

$$Z^* = \bar{S}\frac{Z-Z_G}{S-Z_G}$$

$$\frac{du}{dt} = fV - fV_g - \theta\frac{\partial \pi}{\partial x} + g\frac{(Z^*-\bar{S})}{\bar{S}}\frac{\partial Z_G}{\partial x} - g\frac{Z^*}{\bar{S}}\frac{\partial S}{\partial x} + \left(\frac{\bar{S}}{S-Z_G}\right)^2 \frac{\partial}{\partial Z^*}\left(K_Z^m \frac{\partial u}{\partial Z^*}\right) + \frac{\partial}{\partial x}\left(K_H \frac{\partial u}{\partial x}\right) \quad (1)$$

$$\frac{dv}{dt} = -fu + fU_g + \left(\frac{\bar{S}}{S-Z_G}\right)^2 \frac{\partial}{\partial Z^*}\left(K_Z^m \frac{\partial v}{\partial Z^*}\right) + \frac{\partial}{\partial x}\left(K_H \frac{\partial v}{\partial x}\right) \quad (2)$$

$$\frac{d\theta}{dt} = \left(\frac{\bar{S}}{S-Z_G}\right)^2 \frac{\partial}{\partial Z^*}\left(K_Z \frac{\partial \theta}{\partial Z^*}\right) + \frac{\partial}{\partial x}\left(K_H \frac{\partial \theta}{\partial x}\right) + F_\theta \quad (3)$$

$$\frac{dq}{dt} = \left(\frac{\bar{S}}{S-Z_G}\right)^2 \frac{\partial}{\partial Z^*}\left(K_Z^q \frac{\partial q}{\partial Z^*}\right) + \frac{\partial}{\partial x}\left(K_H \frac{\partial q}{\partial x}\right) + F_q \quad (4)$$

$$\frac{\partial u}{\partial x} + \frac{\partial w^*}{\partial Z^*} = \frac{1}{(S-Z_G)}\left(u\frac{\partial Z_G}{\partial x}\right) - \frac{1}{(S-Z_G)}\left(\frac{\partial S}{\partial t} + u\frac{\partial S}{\partial x}\right) \quad (5)$$

$$\frac{\partial \pi}{\partial Z^*} = -\left(\frac{S-Z_G}{\bar{S}}\right)\frac{g}{\theta} \quad (6)$$

where,

$$\pi = C_p (P/P_0)^{R/C_p},$$

$$\frac{\mathrm{d}}{\mathrm{d}t} = \frac{\partial}{\partial t} + u\frac{\partial}{\partial x} + w^*\frac{\partial}{\partial Z^*},$$

$$w^* = \frac{\bar{S}}{S-Z_G}w - \frac{Z^*}{S-Z_G}\left(\frac{\partial S}{\partial t} + u\frac{\partial S}{\partial x}\right) + \frac{Z^*-\bar{S}}{S-Z_G}\left(u\frac{\partial Z_G}{\partial x}\right)$$

$$\frac{\partial T_s}{\partial t} = \frac{\partial}{\partial Z}\left(K_s\frac{\partial T_s}{\partial Z}\right), \quad -D \leqslant z \leqslant 0, \tag{7}$$

$$\frac{\partial S}{\partial t} = -\frac{1}{\bar{S}}\int_0^{\bar{S}} \frac{\partial}{\partial X}|u(S-Z_G)|\,\mathrm{d}Z^* \tag{8}$$

where $\bar{S}$ and S are the initial and instantaneous heights of the material surface, Z_G the ground elevation above sea level, U_g and V_g the geostrophic components of wind, K_Z and K_H the vertical and horizontal exchange coefficients while the superscripts denote the corresponding variables, T_s and K_s the soil temperature and soil diffusion coefficients respectively.

Eqns. (1) and (2) are the equations of motion. Eqns. (3) through (6) are the energy, moisture, continuity and hydrostatic equations respectively. F_θ and F_q in (3) and (4) are the diabatic source or sink terms of heat and moisture respectively. The heat conduction in the soil is described by (7). The above set of seven equations forms a complete set in seven unknowns (u, v, θ, q, w, π and T_s).

The growth of the PBL (H) during clear days is given by

$$\frac{\partial H}{\partial t} + u\frac{\partial H}{\partial x} = \bar{w} + \frac{1.8w_*^3 + 1.1u_*^3 - 3.3u_*^2 fH}{g\dfrac{H^2\partial\theta^+}{\theta\partial Z^*} + 9w_*^2 + 7.2u_*^2} \tag{9}$$

or,

$$\frac{\partial H}{\partial t} + u\frac{\partial H}{\partial x} = \frac{C_1 u_*^2}{Hf}\left[1 - \left(\frac{C_2 Hf}{u_*}\right)^\alpha\right] \tag{10}$$

where,

$$w_* = \left(-\frac{g}{\theta}u_*\,\theta_*\,H\right)^{1/3},$$

$C_1 + 0.06$, $C_2 = 3.3$ and $\alpha = 3.0$,

u_* and θ_* are the surface layer friction parameters. Other terms have their usual meanings.